Journal of Organometallic Chemistry 891 (2019) 7–11

Contents lists available at ScienceDirect

Journal of Organometallic Chemistry

journal homepage: www.elsevier.com/locate/jorganchem

Theoretical investigation on the palladium-catalyzed diastereoselective oxidative carbocyclization of enallenes assisted by hydroxyl group

Ping Wang [a, b], Jiaying Sun [a, b], Zhangyu Yu [a, b, *], Lingli Han [b, **], Tao Liu [a, b, ***]

[a] School of Chemistry and Chemical Engineering, Qufu Normal University, Qufu, 273165, Shandong Province, PR China
[b] Department of Chemistry and Chemical Engineering, Jining University, Qufu, 273155, Shandong Province, PR China

ARTICLE INFO

Article history:
Received 27 January 2019
Received in revised form
31 March 2019
Accepted 11 April 2019
Available online 13 April 2019

Keywords:
DFT
Enallenes
Diastereoselectivity
Hydroxyl group

ABSTRACT

The reaction mechanisms on the palladium-catalyzed oxidative carbocyclization of enallenes assisted by weak coordination hydroxyl groups have been computationally investigated by employing density functional theory (DFT) calculations. The allyl C-H activation is the rate-determining step and the olefin insertion is the diastereoselectivity-determining step. The calculated results can explain the lower diastereoselectivity obtained in the experiment when the OH group was replaced by OAc or OMe.

1. Introduction

The activation and function of stable C-H bond can provide an approach to synthesize multi-functional drug molecules [1] and functional materials [2,3]. As an efficient catalyst, palladium [4,5] has been widely used in the C-H bond activation [6]. Though the chelation-assisted C-H activation has been reported to be effective in the presence of directing groups, the related study by using weakly coordinating moieties, e.g., hydroxyl group [7], is still limited.

Recently, Bäckvall and coworkers [8] reported the $Pd(OAc)_2$-catalyzed selective carbocyclization of enallene bearing a hydroxyl group (**R1**). By employing B_2pin_2 (**R2**) as partner, the borylated carbocyclization product **P1** was obtained (Scheme 1). As shown in Scheme 1, there are two chiral centers with a 1,3-relationship in the borylated carbocyclization product, while only the single diastereoisomer **P1** was found in this reaction.

The possible reaction mechanisms postulated by Bäckvall et al. [8] are summarized in Scheme 2. The reaction begins with the generation of complex **I** through coordinating of **R1** with catalyst $Pd(OAc)_2$, which is followed by the allyl C-H bond activation to give vinylpalladium complex **II**. Then the ligand exchange of hydroxyl group with olefin gives **III** with excellent diastereoselectivity. The subsequent olefin insertion occurs to afford cyclic complex **IV**. In the following step, transmetalation of **IV** with B_2pin_2 results into intermediate **V**, which would produce the cyclohexene product **P1** through the reductive elimination.

Although the plausible mechanistic pathway has been proposed by Bäckvall et al., several key issues still need to be further discussed. (1) Which steps are rate- and diastereoselectivity-determining? (2) What is the origin of the diastereoselectivity observed experimentally? To address these questions, a theoretical investigation for detailed reaction mechanisms is needed. We have carried out a number of computations on palldium-catalyzed oxidative carbocyclization reaction [9]. Herein, we report our detailed density functional theory (DFT) calculations on the reaction mechanisms, in order to gain insight into the interesting experimental observations and distinct diastereoselectivity. We expect this work would help understand the detailed mechanisms and design new related reactions.

* Corresponding author. School of Chemistry and Chemical Engineering, Qufu Normal University, Qufu, 273165, Shandong Province, PR China.
** Corresponding author. author.
*** Corresponding author. author. School of Chemistry and Chemical Engineering, Qufu Normal University, Qufu, 273165, Shandong Province, PR China.
E-mail addresses: zhy_yu@126.com (Z. Yu), hll_2002@sina.com (L. Han), liutao_2005@126.com (T. Liu).

https://doi.org/10.1016/j.jorganchem.2019.04.010
0022-328X/

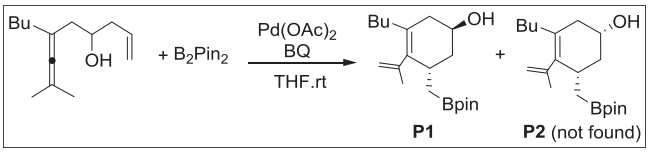

Scheme 1. Bäckvall group's $Pd(OAc)_2$-catalyzed carbocyclization of enallene reaction [8].

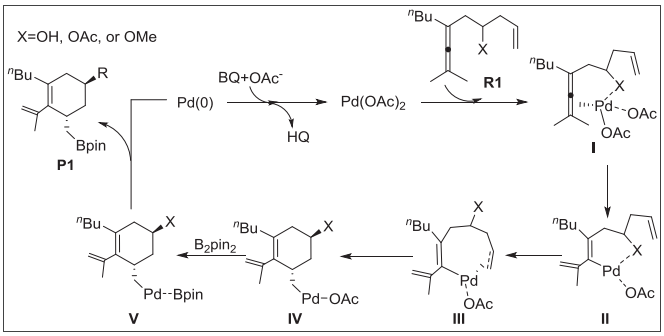

Scheme 2. Possible reaction mechanisms proposed by Bäckvall and coworkers.

2. Computational details

All structures were optimized at the B3LYP [10]/BSI level (BSI designates the basis set combination of LanL2DZ [11] for Pd atom, and 6-31G (d,p) for other atoms) in the gas phase. Harmonic vibrational frequencies were also calculated at the same level of theory to identify all stationary points as minima (zero imaginary frequencies) or transition states (one imaginary frequency). Intrinsic coordinate reaction (IRC) [12] calculations were carried out to examine the connectivity of a transition state with its backward and forward minima when necessary. Natural bond orbital (NBO) analyses were performed at the B3LYP [10]/BSI level on selected systems with the NBO code included in Gaussian 09 [13]. The energetic results were then further refined by single-point calculations at the M06/BSII [14] level with solvation effects accounted for by the SMD [15] solvent model using 1,2-dichloroethane (DCE) [16] as solvent according to the experimental conditions, where BSII denotes the basis set combination of SDD [17] for Pd atom and 6–311++G (d,p) for the remaining atoms. In all of the figures that contain energy diagrams, calculated relative Gibbs free energies are presented. For reference, relative enthalpic energies are also given in parentheses. All the energies are given in kcal/mol. Unless otherwise stated, Gibbs free energies are used for the discussion of reaction mechanisms. All the calculations were performed with the Gaussian 09 [13] software package.

3. Results and discussion

In this reaction, the substrate **R1** could coordinate with catalyst $Pd(OAc)_2$ to generate some species (Scheme 3). According to our calculations, **1c** is calculated to be the most stable one.

The free energy diagrams for the allyl C-H activation process of **R1** catalyzed by $Pd(OAc)_2$ are shown in Fig. 1. The important structures are listed in Fig. 2. The reaction would begin with the coordination of **R1** to $Pd(OAc)_2$ to form intermediate **1c**. This step is energetically favorable and exergonic by 13.8 kcal/mol. Then, **1c** is isomerized to intermediate **1a**. Subsequently, the sp^3 C-H bond activation process occurs with the base-assisted concerted metalation/deprotonation (CMD) mechanism through the six-membered ring transition state **TS1** to afford the intermediate **2**, requiring the free energy barrier of 22.9 kcal/nol. With the releasing of HOAc, a more stable intermediate **3** is formed.

As shown in Fig. 3, **3** could become intermediate **4** through the

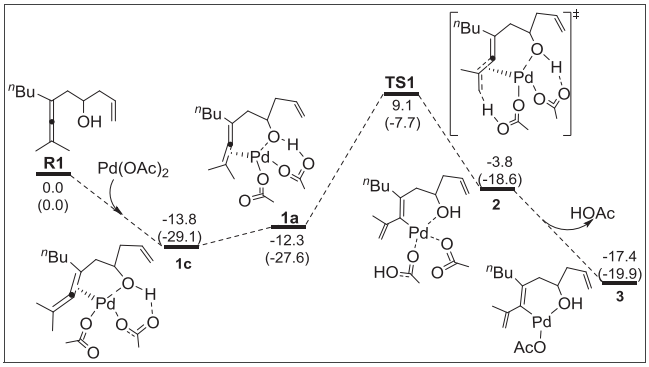

Fig. 1. Free energy diagrams for the C-H activation process of **R1** catalyzed by $Pd(OAc)_2$. The relative free energies and relative enthalpic energies (in parentheses) are given in kcal/mol.

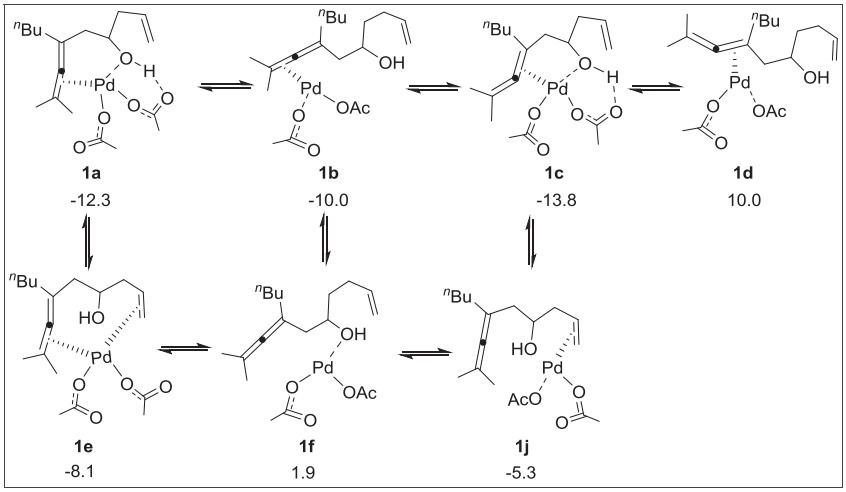

Scheme 3. Possible $Pd(OAc)_2$-**R** coordination isomers and their relative stability. The relative free energies are given in kcal/mol, where the free energy of [$Pd(OAc)_2$ + **R**] is set to zero reference point.

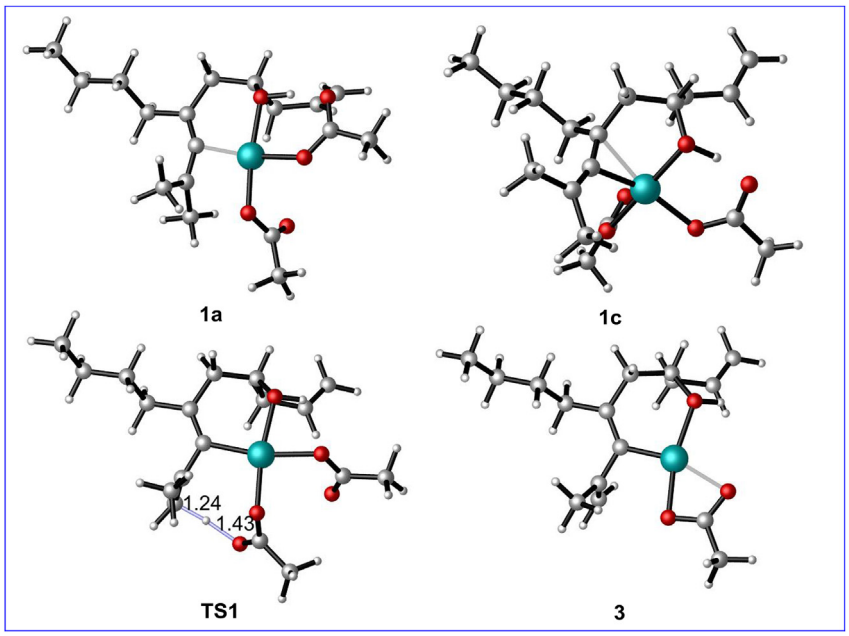

Fig. 2. Optimized geometries of key intermediates and transition states involved in the reaction mechanism shown in Fig. 1. Bond distances are given in Å.

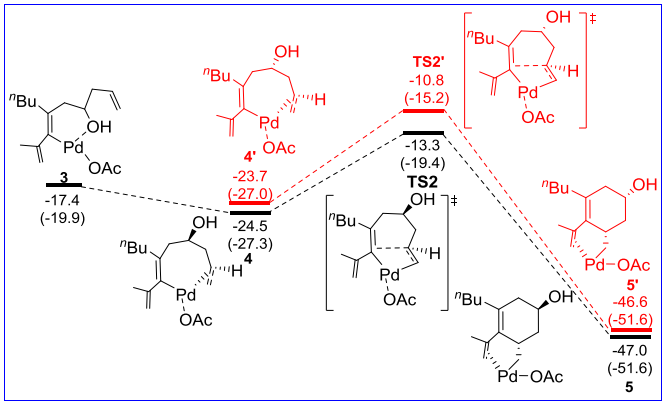

Fig. 3. Free energy diagrams for the olefin insertion step catalyzed by $Pd(OAc)_2$. The relative free energies and relative enthalpic energies (in parentheses) are given in kcal/mol.

ligand exchange. The subsequent olefin insertion into Pd-C bond occurs to transform into intermediate **5** via the transition state **TS2** with the activation barriers of 11.2 kcal/mol **4′**, the isomer of **4**, could also undergo olefin insertion to afford intermediate **5'** by overcoming the free energy of 13.7 kcal/mol (Fig. 3). The inaccessible pathways for other two isomers of **4** were also calculated (Figs. S1 and S2 in Supporting Information) (see Fig. 4).

With the participation of another substrate **R2** (B_2pin_2), intermediate **6** is obtained (Fig. 5). Then **6** isomerizes into intermediate **7** by overcoming a facile barrier of 2.5 kcal/mol. Subsequently, transmetallation occurs to give a more stable intermediate **8** via the B-B activation transition state **TS4**, requiring the barrier of 12.7 kcal/mol. Finally, **8** undergoes the reductive elimination to generate the product-coordinated complex **9**, accompanied with the catalyst $Pd(OAc)_2$ regenerating. The corresponding pathway to lead to another product-coordinated diastereoisomer **9'** is shown in Fig. 5 (red line) (see Fig. 6).

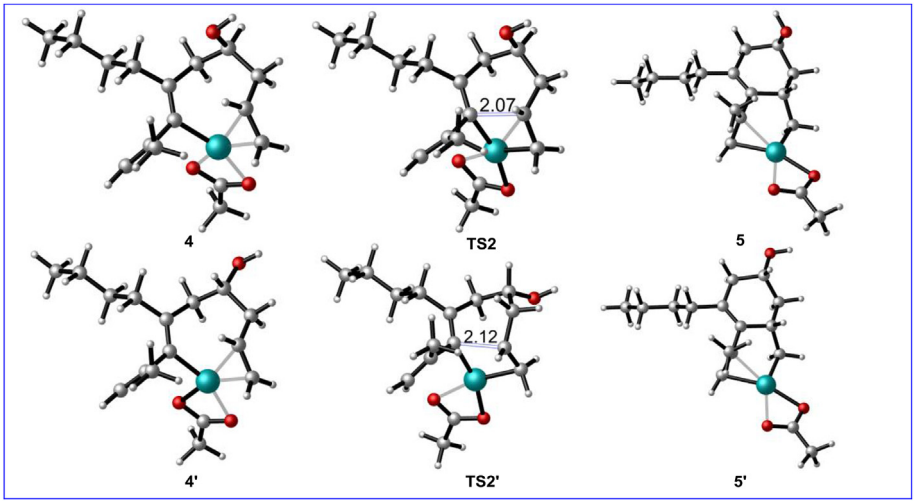

Fig. 4. Optimized geometries of key intermediates and transition states involved in the reaction mechanism shown in Fig. 3. Bond distances are given in Å.

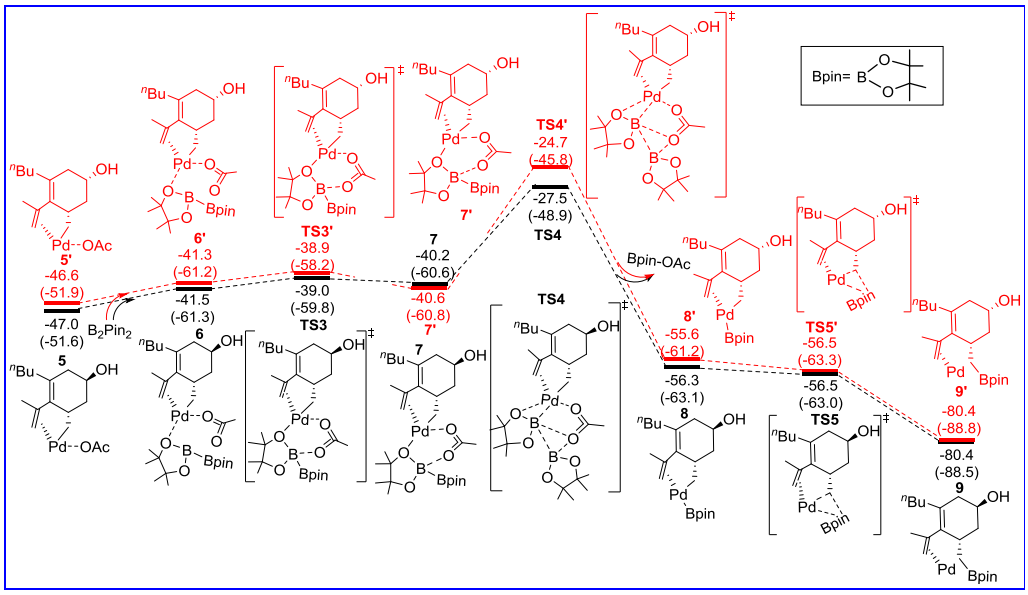

Fig. 5. Free energy diagram for the transmetallation and reduction elimination processes catalyzed by $Pd(OAc)_2$. The relative free energies and relative enthalpic energies (in parentheses) are given in kcal/mol.

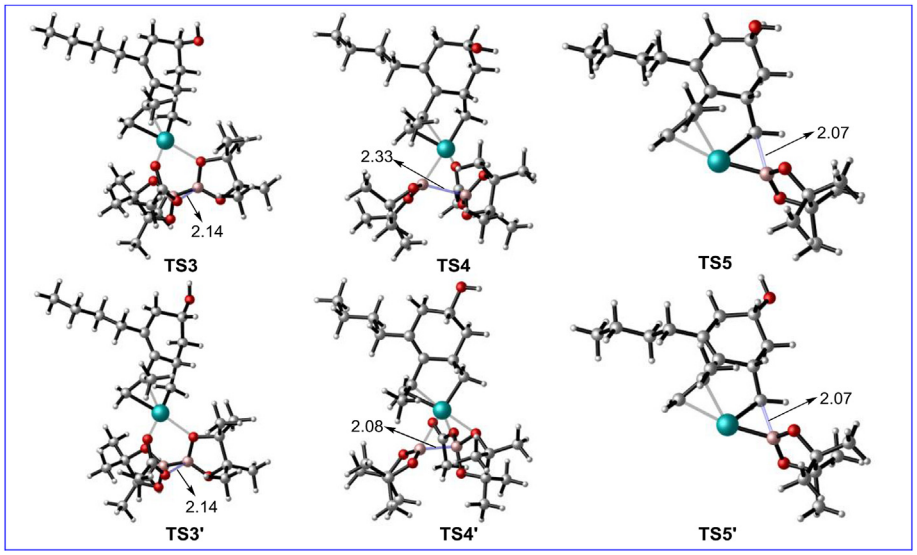

Fig. 6. Optimized geometries of key intermediates and transition states involved in the reaction mechanism shown in Fig. 5.

Putting Figs. 1, 3 and 5 together, it can be found that the allyl C-H activation is the rate-determining step and the overall free energy barrier is 22.9 kcal/mol. The olefin insertion controls the diastereoselectivity of the reaction. The reasons are as follows: First, the step is highly exoergonic by 29.6 kcal/mol, being irreversible. Second, the relative energies of insertion transition states (**TS2** and **TS2′**) are much higher than those of B-B activation transition states (**TS4** and **TS4'**). Thus, as long as the olefin insertion occurs, the formed intermediate easily undergoes the subsequent steps to generate the products.

The corresponding diastereoselectivity-determining steps are given in Scheme 4 when the directing OH group is substituted by OAc or OMe group. The relative energy differences between the olefin insertion transition states in the two reactions (1.1 and 0.8 kcal/mol) are closer than that by using OH group (2.5 kcal/mol), which is consistent with the experimental observations of the lower diastereoselectivity.

4. Conclusions

With the aid of the DFT calculations, we have investigated the reaction mechanisms of high-selective palladium-catalyzed oxidative carbocyclization of enallenes assisted by weak coordination hydroxyl groups. Our calculations have confirmed the mechanism proposed by Bäckvall et al. The reaction includes four main steps: C-H activation, carbocyclization, transmetalation, and reduction elimination. The allyl C-H activation is the rate-determining step and the olefin insertion is the diastereoselectivity-determining step. The calculated results can explain the lower diastereoselectivity obtained in the experiment when the OH group was replaced by OAc or OMe.

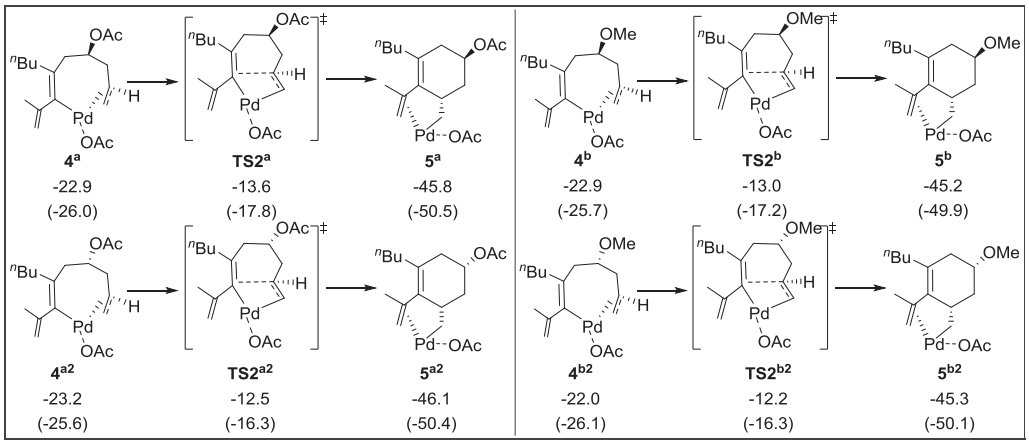

Scheme 4. The diastereoselectivity-determining steps catalyzed by $Pd(OAc)_2$ with the directing group of OAc or OMe group. The relative free energies and relative enthalpic energies (in parentheses) are given in kcal/mol.

Acknowledgements

This work was jointly supported by the National Natural Science Foundation of China (No. 21803024), the Natural Science Foundation of Shandong Province (No. ZR2018LB016), and the Talent Team Culturing Plan for Leading Disciplines of University in Shandong.

Appendix A. Supplementary data

Supplementary data to this article can be found online at https://doi.org/10.1016/j.jorganchem.2019.04.010.

References

[1] (a) K. Shailubhai, Leuk. Res. 31 (2007) 9–10;
(b) X. Yang, Y. Wang, X. Huang, Y. Ma, J. Mater. Chem. 21 (2011) 3448–3454;
(c) D. Bacinello, G. Elisabeth, D. Taton, K.C. Tam, L. Sébastien, Eur. Polym. J. 62 (2015) 363–373.
[2] (a) O. Ikkala, G.T. Brinke, Sci 295 (2002) 2407–2409;
(b) N.V. Tsarevsky, Nat. Chem. 1 (2009) 276–288;
(c) R. Costi, A.E. Saunders, U. Banin, Angew. Chem. Int. Ed. 49 (2010) 4878–4897.
[3] (a) R. Zimmer, C.U. Dinesh, E. Nandanan, F.A. Khan, Chem. Rev. 100 (2000) 3067–3126;
(b) J.A. Marshall, Chem. Rev. 31 (2000) 3163–3186;
(c) L.K. Sydnes, Chem. Rev. 103 (2003) 1133;
(d) S. Ma, Aldrichim Acta 40 (2007) 91–102;
(e) S. Yu, S. Ma, Angew. Chem. Int. Ed. 51 (2012) 3074–3112.
[4] (a) L.J. Goossen, D. Koley, T. Hermann, Organometallics 24 (2005) 2398–2410;
(b) R. Suleiman, V. Polo, B.E. Ali, RSC Adv. 6 (2016) 8440–8448;
(c) R. Suleiman, A. Ibdah, B.E. Ali, J. Organomet. Chem. 696 (2011) 2355–2363;
(d) Y. Kaya, C. Lcsel, V.T. Yilmaz, J. Organomet. Chem. 752 (2014) 83–90.
[5] (a) P. Surawatanawong, Y. Fan, M.B. Hall, J. Organomet. Chem. 693 (2008) 1552–1563;
(b) P. Surawatanawong, M.B. Hall, Organometallics 27 (2008) 6222–6232.
[6] (a) D.A. Colby, R.G. Bergman, J.A. Ellman, Chem. Rev. 110 (2010) 624–655;
(b) D.A. Colby, G.M. Ferrence, T.D. Lash, Angew. Chem. Int. Ed. 43 (2004) 1346–1349;
(c) S. Hwan, Kim, Ji Young, Chem. Soc. Rev. 40 (2011) 5068–5083;
(d) K.R. Campos, J. Cheminf. 36 (2007) 1069–1084.
[7] (a) H. Miyabe, Y. Yousuke, T. Yoshiji, J. Org. Chem. 37 (2010) 573–582;
(b) J. Staroscik, B. Rickborn, J. Org. Chem. 37 (1972) 738–740;
(c) D. Vollhardt, V.B. Fainerman, J. Phys. Chem. B 108 (2004) 297–302;
(d) J.A. Staroscik, B. Rickborn, J. Org. Chem. 37 (1972) 738–740;
(e) J.F. Baker, R.T. Blickenstaff, J. Org. Chem. 40 (1975) 1579–1586.
[8] D. Posevins, Y. Qiu, J.E. Bäckvall, J. Am. Chem. Soc. 140 (2018) 3210–3214.
[9] (a) L. Han, T. Liu, Org. Biomol. Chem. 15 (2017) 5055–5061;
(b) X. Zheng, L. Nie, Y. Li, S. Liu, F. Zhao, X. Zhang, X. Wang, T. Liu, RSC Adv. 7 (2017) 5013–5018;
(c) Y. Li, S. Miao, Z. Yu, T. Liu, J. Organomet. Chem. 853 (2017) 143–148;
(d) J. Zhang, C. Shan, K. Lv, L. Zhu, Y. Li, T. Liu, Y. Lan, ChemCatChem 11 (2019) 1228–1237.
[10] (a) A.E. Aliev, D. Courtier-Murias, J. Mol. Struct. Theochem. 893 (2009) 1–5;
(b) P. Winget, T. Clark, J. Comput. Chem. 25 (2004) 725–733;
(c) D.V. Chachkov, O.V. Mikhailov, Russ. J. Org. Chem. 54 (2009) 1952–1956;
(d) H. Kruse, L. Goerigk, S. Grimme, J. Org. Chem. 77 (2012) 10824–10834;
(e) Y. Yang, Y. Liu, P. Lv, R. Zhu, C. Liu, D. Zhang, J. Org. Chem. 83 (2018) 2763–2772;
(f) G. Molteni, A. Ponti, J. Org. Chem. 82 (2017) 10710–10714.
[11] (a) X. Ji, P. Zhang, W. Wei, H. Zhang, B. Xia, J. Organomet. Chem. 862 (2018) 40–52;
(b) S. Esmaielzadeh, E. Zarenezhad, Acta Chim. Slov. 65 (2018) 416–428;
(c) Q. Wei, Y. Dai, C. Chen, L. Shi, Z. Si, Y. Wan, Q. Zuo, D. Han, Q. Duan, J. Mol. Struct. 1171 (2018) 786–792;
(d) M.E. Belghiti, S. Echihi, A. Mahsoune, Y. Karzazi, A. Dafali, I. Bahadur, J. Mol. Liq. 261 (2018) 62–75;
(e) A.M. Mansour, O.R. Shehab, Inorg. Chim. Acta 480 (2018) 159–165.
[12] (a) B. H Cadirci, Int. J. Hydrogen Energy 43 (2018) 18001–18006;
(b) K. Yoshizawa, Y. Shiota, T. Yamabe, J. Chem. Phys. 111 (1999) 538–545;
(c) S. Maeda, Y. Harabuchi, M. Takagi, K. Suzuki, T. Lchino, Y. Sumiya, K. Sugiyama, Y. Ono, J. Comput. Chem. 39 (2018) 233–251;
(d) Y. Ni, Y. Pan, J. Zhang, X. Gu, X. Pan, J. Jiang, Q. Wang, Comput. Theor. Chem. 1135 (2018) 11–17;
(e) J.M. Burns, Org. Biomol. Chem. 16 (2018) 1828–1836.
[13] M.J. Frisch, G.W. Trucks, H.B. Schlegel, G.E. Scuseria, M.A. Robb, J.R. Cheeseman, G. Scalmani, V. Barone, B. Mennucci, G.A. Petersson, H. Nakatsuji, M. Caricato, X. Li, H.P. Hratchian, A.F. Izmaylov, J. Bloino, G. Zheng, J.L. Sonnenberg, M. Hada, M. Ehara, K. Toyota, R. Fukuda, J. Hasegawa, M. Ishida, T. Nakajima, Y. Honda, O. Kitao, H. Nakai, T. Vreven, J.A. Montgomery Jr., J.E. Peralta, F. Ogliaro, M. Bearpark, J.J. Heyd, E. Brothers, K.N. Kudin, V.N. Staroverov, R. Kobayashi, J. Normand, K. Raghavachari, A. Rendell, J.C. Burant, S.S. Iyengar, J. Tomasi, M. Cossi, N. Rega, N.J. Millam, M. Klene, J.E. Knox, J.B. Cross, V. Bakken, C. Adamo, J. Jaramillo, R. Gomperts, R.E. Stratmann, O. Yazyev, A.J. Austin, R. Cammi, C. Pomelli, J.W. Ochterski, R.L. Martin, K. Morokuma, V.G. Zakrzewski, G.A. Voth, P. Salvador, J.J. Dannenberg, S. Dapprich, A.D. Daniels, O. Farkas, J.B. Foresman, J.V. Ortiz, J. Cioslowski, D.J. Fox, Gaussian 09, Revision D.01, Gaussian Inc., Wallingford CT, 2009.
[14] (a) F. Huang, J. Jiang, M. Wen, Z. Wang, J. Theor. Comput. Chem. 13 (2014) 1350074;
(b) R.V. Belzen, C.J. Elsevier, A. Dedieu, N. Veldman, Organometallics 22 (2003) 722–736;
(c) C.A. Bayse, Inorg. Chem. 45 (2006) 2199–2202.
[15] (a) A.V. Marenich, C.J. Cramer, D.G. Truhlar, J. Phys. Chem. 113 (2009) 6378–6396;
(b) D.G. Fedorov, Chem. Phys. Lett. 702 (2018) 111–116;
(c) K. Aidas, J. Comput. Chem. 36 (2015) 2158–2167;
(d) J.J. Guerard, J.S. Arey, J. Chem. Theory Comput. 9 (2013) 5046–5058;
(e) M.W. Lehmann, D.H. Evans, Anal. Chem. 71 (1999) 1947–1950;
(f) L. Castro, E. Kirillov, O. Miserque, A. Welle, L. Haspeslagh, J.F. Carpentier, L. Maron, ACS Catal. 5 (2015) 416–425;
(g) K. Jana, B. Ganguly, J. Phys. Chem. A 118 (2014) 9753–9761.
[16] (a) N.A. Murugan, H. Ågren, J. Phys. Chem. B 113 (2009) 3257–3263;
(b) M. Itagaki, H. Fukushima, H. Lnoue, K. Watanabe, J. Electroanal. Chem. 504 (2001) 96–103;
(c) B.L. Mcclain, D. Ben-Amotz, J. Phys. Chem. B 106 (2002) 7882–7888;
(d) D.S. Brandt, Forensic Sci. Int. 178 (2008) 162–170.
[17] (a) G. Igel-Mann, H. Stoll, H. Preuss, Mol. Phys. 65 (1988) 1321–1328;
(b) D. Andrae, U. Haeussermann, M. Dolg, H. Stoll, H. Preuss, Theor. Chim. Acta 77 (1990) 123–141;
(c) G.V. Barnett, V.I. Razinkov, B.A. Kerwin, T.M. Laue, A.H. Woodka, P.D. Butler, T. Perevozchikova, C.J. Roerts, J. Phys. Chem. B 119 (2015) 5793–5804;
(d) Y. Liu, C. Sun, S. Zhang, Theor. Chem. Acc. 132 (2013) 1–10.